Bioactive Materials 8 (2022) 355–367

Contents lists available at ScienceDirect

Bioactive Materials

journal homepage: www.sciencedirect.com/journal/bioactive-materials

Gastrodin modified polyurethane conduit promotes nerve repair via optimizing Schwann cells function

Hongcai Yang [a,1], Qing Li [b,1], Limei Li [b,1], Shaochun Chen [c], Yu Zhao [b], Yingrui Hu [b], Lu wang [b], Xiaoqian Lan [a], Lianmei Zhong [a,**], Di Lu [b,*]

[a] Yunnan Key Laboratory of Stem Cell and Regenerative Medicine, Department of Neurology, The First Affiliated Hospital, Kunming Medical University, Kunming, 650500, China
[b] Yunnan Key Laboratory of Stem Cell and Regenerative Medicine, Science and Technology Achievement Incubation Center, Kunming Medical University, Kunming, 650500, China
[c] The School of Rehabilitation, Kunming Medical University, Kunming, 650500, China

ARTICLE INFO

Keywords:
Gastrodin/PU
SCs biological behavior
Anti-inflammatory
Peripheral nerve regeneration

ABSTRACT

Peripheral nerve regeneration and functional recovery remain a major clinical challenge. Nerve guidance conduit (NGC) that can regulate biological behavior of Schwann cells (SCs) and facilitate axonal regeneration through microenvironmental remodeling is beneficial for nerve regeneration and functional recovery. Gastrodin, a main constituent of a Chinese traditional herbal medicine, has been known to display several biological and pharmacological properties, especially antioxidative, anti-inflammatory and nerve regeneration. Herein, polyurethane (PU) NGCs modified by different weight ratio of Gastrodin (0, 1 and 5 wt%) were designed for sequential and sustainable drug release, that created a favorable microenvironment for nerve regeneration. The scaffold showed suitable pore structure and biocompatibility *in vitro*, and evidently promoted morphological and functional recovery of regenerated sciatic nerves *in vivo*. Compared to the PU and 1%Gastrodin/PU scaffolds, the 5%Gastrodin/PU significantly enhanced the proliferation, migration and myelination of SCs and up-regulated expression of neurotrophic factors, as well as induction of the differentiation of PC12 cells. Interestingly, the obvious anti-inflammatory response was observed in 5%Gastrodin/PU by reduced expression of TNF-α and iNOS, which also evidenced by the few fibrous capsule formation in the subcutaneous implantation. Such a construct presented a similarity to autograft *in vivo* repairing a 10 mm sciatic nerve defects. It was able to not only boost the regenerated area of nerve and microvascular network, but also facilitate functional axons growth and remyelination, leading to highly improved functional restoration. These findings demonstrate that the 5%Gastrodin/PU NGC efficiently promotes nerve regeneration, indicating their potential for use in peripheral nerve regeneration applications.

1. Introduction

Peripheral nerve injury (PNI) is an intractable clinical problem bringing heavy burdens to patients, due to its high incidence and unsatisfactory treatment. Severe PNI mainly causes sensory and locomotor dysfunction that can result in complete paralysis of the affected limb, and development of intractable neuropathic pain, which impacts on a patients' quality of life [1]. Although the peripheral nervous system (PNS) has an intrinsic ability to repair, regeneration by end-to-end suture only occurs for short segmental nerve defects and under ideal conditions, axons of the transected nerve regenerate vigorously to the extent limited by the size of the nerve gap and scar tissue formation [2]. Herein, current interventions for the large segmental nerve defects (greater than ~10 mm) typically require the bridging by nerve grafts [3]. Autograft nerve transplantation with only less than 50% success rate remains the gold standard surgical therapy [4]. Despite

Peer review under responsibility of KeAi Communications Co., Ltd.
* Corresponding author.
** Corresponding author.
E-mail addresses: 13888967787@163.com (L. Zhong), ludi20040609@126.com (D. Lu).
[1] These authors contribute equally to this work.

https://doi.org/10.1016/j.bioactmat.2021.06.020
Received 20 February 2021; Received in revised form 18 June 2021; Accepted 18 June 2021
Available online 2 July 2021

considerable improvements in the application of microsurgery, functional recovery following such therapy are far from complete solving. Nerve guidance conduits (NGCs), enabling guided cell growth and axon extension to promote peripheral nerve regeneration and function restoration, have emerged as a potential alternative to autografts to bridge the gap between injured peripheral nerve stumps [5]. NGCs can prevent scar formation, but usually lack guidance cues like Schwann cells (SCs) and therapeutic levels of neurotrophic factors. There is considerable need for improved microenvironment of the native tissue and improved nerve tissue-engineering graft substitutes [6].

Unlike nervous tract in the central nervous system (CNS), injured peripheral nerves exhibit the ability to regenerate largely due in part to the supportive population of SCs, which are primary neuroglial cells in the PNS [7]. SCs play a key role in peripheral nerve repair not only in the early clearance of debris and control of inflammation but also in axon growth and myelination [8]. SCs are unique in their capacity to de-differentiate, re-enter the cell cycle, and subsequently myelinate regenerating axons [9]. Proliferating mature SCs produce growth factors, cytokines, growth-associated proteins, axonal ligands and establishing a supportive growth matrix in the microenvironment after PNI [10], which facilitate axonal remyelination and peripheral nerve regeneration [11,12]. It has been observed that exogenously administered neuroglial cell line-derived neurotrophic factor (GDNF) increases both the number and myelination of regenerating axons [13]. This is due to effects of GDNF signaling both on regenerating nerve fibers and on Schwann and inflammatory cells, and SCs migration is thought to precede and promote axon elongation into repair sites [14]. Brain-derived neurotrophic factor (BDNF) is a member of the neurotrophin family and enhances myelination in SCs, promotes neuronal survival and neurite outgrowth, and prevents neural death [15,16]. Studies indicate that BDNF exerts regrowth-promoting effects on nerve after sciatic nerve injury and is closely related to motor recovery following PNI [17,18]. Without either neurite outgrowth matrix or neurotrophic factors, regeneration will either not occur or be dysfunction [19]. In this regard, understanding the synergistic effects on nerve regeneration involved in this complex crosstalk between growth promoting matrix and neurotrophin, which describes a challenge to develop more accessible NGCs for upregulating SCs biological behavior to repair injured nerves.

In the pursuit of an effective nerve conduit, constructing the neurovascular microenvironment of scaffold materials is associated with stimulating repair process [20]. One reason for limited regeneration is insufficient vascularization around or inside the implant [21], resulting in inadequate nutrient supply and gas exchange to support nerve growth. In addition, implants may not provide the appropriate microenvironment for nerve regeneration [22]. Therefore, implants should be endowed with both angiogenic and neuroregenerative capacity for optimum clinical efficacy. For example, scaffolds pre-seeded with induced stem cells [23], and immobilized angiogenic factors or genes [24], have been developed for various applications in tissue engineering and regenerative medicine. While substantial progress has been achieved in scaffold vascularization, there are still insufficient data for clinical application. The previous study proposed an acellular nerve scaffolds based on a VEGF-heparin sustained release system could achieve early vascularization and restore blood supply in the nerve graft area. However, its neuroregenerative effect was not as good as that of autografting, indicating a limitation in the use of a single factor in repairing nerve injury [25]. Other studies showed that combined use of neurotrophic peptide sequence and other peptide motifs derived from growth factors, such as NGF and VEGF, promoted nerve regeneration [26]. Therefore, efforts to establish synergetic scaffolds harboring function to simulate effects of the angiogenic and neurotrophic factors have been devoted in the search for new therapeutic approachs.

As a polyfunctional biomaterial for tissue-engineered scaffold, polyurethane (PU) NGC has shown surprising results on axonal regeneration and muscle functional recovery of injured neural tissues [27]. Nevertheless, regenerative process mediated by NGCs always brings with inflammatory response [28]. A prolonged inflammatory response is considered as the pathogenesis of negative symptoms after PNI or other nerve diseases [29], and shows a negative effect on functional recovery and some anti-inflammatory factors are verified to be beneficial for nerve regeneration *in vivo* [30]. Gastrodin, a bioactive component of an ancient Chinese herb Tianma (Gastrodinelata B1), has been known to neuroprotective and anti-inflammatory effects due to cell protection from reactive oxygen species and reactive nitrogen species [31]. Compelling evidence have identified its effects not only on scavenging free radicals and inhibiting apoptosis by regulating expression of proinflammatory cytokines such as TNF-α and IL-1β [32], but also stimulating release of BDNF [33]. Utilizing the potential anti-inflammatory [34] and neuroprotective effect of Gastrodin [35], our laboratory have designed and fabricated the Gastrodin functionalized PU nerve films, which showed hydrophilicity, interconnected porous structure, good flexibility and compatible neurite extension for PC12 cells [36]. Furthermore, we reported recently that Gastrodin-functionalized PU elevated angiogenesis without obvious inflammatory response during subcutaneous implantation [37]. Therefore, NGCs loaded with Gastrodin may be a potential candidate coupled with angio- and neurogenesis for facilitating functional recovery.

It is possible, therefore, that a functional Gastrodin/PU NGC is designed for sequential and sustainable drug release, which creates a favorable microenvironment for nerve regeneration. To test this possibility, we investigated the potential regenerative role of functional Gastrodin/PU NGC and found that Gastrodin/PU NGC efficiently promotes nerve regeneration, indicating their potential for use in peripheral nerve regeneration applications.

2. Materials and methods

2.1. Fabrication of Gastrodin/PU NGCs

2.1.1. Reagents

Gastrodin (purity > 99.0%) was purchased from Kunming Pharmaceutical Co. Ltd., China. Isophorone diisocyanate (IPDI), Lysine ethyl ester dihydrochloride (Lys·OEt–2HCl) and Poly (Ɛ-caprolactone)2000 (PCL2000) were purchased from Aladdin Co. Ltd., China. The source of other chemicals of AR grade was purchased from Tianjin Fengchuan Chemical Reagent Technology (China).

2.1.2. Synthesis of Gastrodin/PU polymers

PU polymers with different concentration gradients of Gastrodin were successfully synthesized using the *in situ* polymerization method [36]. Primarily, PCL2000 and IPDI, 30.00 g and 7.80 g, respectively, were mixed in a 250 ml three-necked flask under nitrogen continuously and heated at 70 °C, stirred for 4 h with 4 drops SnOct as catalyzer to obtain the prepolymer. Posteriorly, 3.70 g of Lys·OEt–2HCl was applied to extend the prepolymer. After stirring for 2 h, different doses of Gastrodin were added into the mixture to synthesize different concentration gradient polymers. Finally, the resultant polymer was cured at 90 °C. According to the theoretical weight ratio of Gastrodin in polymer chain (set as 0, 1, and 5 wt%), the samples were named as PU, 1%Gastrodin/PU, and 5%Gastrodin/PU, respectively.

2.1.3. Preparation of NGCs

The NGCs were prepared using the dipping-leaching method [6]. In brief, the samples were dissolved in 1, 4-dioxane and twice of NaCl (by weight) particles (<50 μm) as porogen were added into the solution and mixed thoroughly. Stainless steel wires (*Φ*1.28 mm) were dipped vertically and removed from the suspensions for a total three cycles. After air drying 24 h to eliminate solvent, the conduit was taken down from the steel wire. And the NaCl particles were dissolved away from the conduit by immersion in deionized water under vacuum for 48 h to obtain porous NGCs.

2.2. Characterization

2.2.1. Morphology

Microstructure characterization of the NGCs was observed under scanning electron microscopy (SEM, FEI Quanta-200, Switzerland) at an accelerating voltage of 10 kV. Before morphology observation, the specimens were sputter-coated with a 7 nm layer of gold. The average pore sizes of the scaffold section surfaces were measured using an Image J software from the SEM photographs.

2.2.2. Degradation study

The specimens (~0.2 g) were immersed in tubes containing 3 ml 0.1 M NaOH solution and placed in an incubator at 37 °C. Each group was prepared in quintuplicate. The solution was refreshed every week until the 6th week.

2.2.2.1. Mass loss. Specimens were collected and gently rinsed 3 times with distilled water at 1, 2, 4, 6 weeks, followed by oven drying to a constant weight. The mass loss of the degraded samples was quantified by Equation (1) [38].

$$\text{Mass loss } (\%) = [(W_0 - W_1) / W_0] \times 100\% \quad (1)$$

where W_0 and W_1 represent the weights of scaffolds before and after degradation, respectively.

2.2.2.2. Gastrodin release. The Gastrodin released from polyurethane was quantified by high performance liquid chromatography (HPLC; Shimadzu, Kyoto, Japan). The collected degradation liquid was filtered through a 0.22 μm filter, separated on a C18 column (250 mm × 4.6 mm, 5 μm, USA) using a mobile phase composed of solvent A (0.05% phosphoric acid aqueous solution) and solvent B (acetonitrile). The ratio of solvent A to solvent B is 97:3. The sample injection volume was 10 μl and the flow rate was 0.8 ml/min. The detection of Gastrodin was set at 220 nm, and a calibration curve of Gastrodin was obtained under the same conditions (Fig.S1).

2.3. In vitro cell culture tests

2.3.1. SCs growth on the scaffolds

Investigations of cell biological function on the nerve guide scaffolds were performed using SCs (Beina, shanghai, China) *in vitro*. SCs were cultured in 75 mm^2 cell culture flask in Dulbecco's modified Eagle's medium (DMEM, HyClone, USA) supplemented with 10% fetal bovine serum (FBS, Gibco, USA) and incubated at 37 °C, 5% CO_2. The culture medium was renewed every 2 days.

After sterilized with γ-ray irradiation with 15 kGy, the scaffolds were incubated with SCs (1×10^5 cells/well) in 12-well plates for 3 days. The SEM was performed to characterize the growth situation of cells on the scaffolds. Samples were washed twice with PBS, fixed in 3% glutaraldehyde buffer for 1 h, then rinsed by PBS and dehydrated in gradient ethanol series. Dried samples with the cell presence were metalized with a thin layer of gold and performed by SEM with an accelerating voltage of 10 kV. Labeling of cells for immunofluorescence observation involved the use of nerve growth factor (NGF). DAPI (Abcam, USA) was applied to stain the cell nucleus followed by imaging under an optical microscope (BX53, Olympus, Japan).

2.3.2. Cell migration assay

SCs (2×10^5 cells/well) were seeded onto scaffolds in 6-well plates and cultured until ~90% confluence. A scratch was induced using a sterile 200 μl pipet tip, and the cell debris was washed with PBS. Then, fresh medium without FBS was added to the wells. The cell migration propensity was imaged after 0, 24 and 48 h. The wounded areas were measured by Image J and quantified by Equation (2).

$$\text{Wounded} - \text{healing rate } (\%) = [(S_1 - S_0) / S_0] \times 100\% \quad (2)$$

where S_0 and S_1 represent the area of cells before and after migration, respectively.

2.3.3. RT-qPCR and western blotting

In order to explore the effect of scaffolds on SCs function, SCs (2×10^5 cells/well) were seeded onto scaffolds in 6-well plates for 3 days. The gene expression levels of neuronal cellular adhesion molecules (NCAM), GDNF and BDNF were measured by RT-qPCR. The protein expressions of NCAM, early growth response 2 (EGR2), NGF, GDNF and BDNF were evaluated using Western blotting. The process was reported in the SI.

2.3.4. PC12 cell differentiation

The bioactivity of growth factors secreted by SCs on scaffolds was evaluated based on PC12 cell differentiation. Briefly, PC12 cells (2.0×10^4 cells/well) were seeded into 12-well plates and incubated for 24 h. Then the medium was replaced with conditioned medium collected from SCs cultured on scaffolds for 3 days and supplemented with 2.5% FBS. The culture with normal medium was used as controls. After 3 days of culture, differentiated PC12 cells were fixed with 4% paraformaldehyde and stained with β-Tubulin-III for cytoplasm and DAPI for nucleus. The stained cells were observed with an optical microscope. The neurite length and percentage of differentiated cells were calculated using Image J software. Furthermore, the effect of scaffolds/SCs conditional medium on the FAK expression of PC12 was assessed by RT-qPCR analysis.

2.3.5. Anti-inflammatory properties

To evaluate the anti-inflammatory properties of scaffolds, RAW264.7 cells (2×10^4 cells/well) were seeded onto the various scaffolds in 12-well plates in DMEM supplemented with 10% FBS. After incubated for 3 days (37 °C, 5% CO_2), the cells were fixed with 4% paraformaldehyde and stained with iNOS for cytoplasm and DAPI for nucleus. The stained cells were then observed with an optical microscope. Meanwhile, gene expression of iNOS and TNF-α was quantified using RT-qPCR analysis. Supernatant of medium was collected and assayed to measure the content of TNF-ɑ using a TNF-ɑ Elisa kit (Nanjing jiancheng, China) according to the manufacturer's instructions.

2.4. Animal experiment

Sprague-Dawley (SD) rats (male, 200–220 g) supplied by the Experimental Animal Center of Kunming Medical University (Kunming, China) were used for *in vivo* experiments. The animal experiments were approved by the local institution of Animal Experimental Ethics Committee of Experimental Animal Center of Kunming Medical University in compliance with international ethics guidelines and regulations. Animals were anesthetized with sodium pentobarbital (30 mg/kg).

2.4.1. Anti-inflammatory response of the scaffolds in the subcutaneous embedding model

27 rats were randomly divided into PU, 1%Gastrodin/PU and 5% Gastrodin/PU groups. Sterilized discs (Φ13 mm × 2 mm) were transplanted into the dorsal subcutaneous pocket symmetrically per rat. After 3, 7, 14 days of implantation, the samples with surrounding tissues were harvested and fixed with 4% paraformaldehyde solution for histological (Masson) and immunofluorescent (TNF-α, CD31) staining. To evaluate the toxicity of scaffolds, routine blood and blood biochemistry test at 14 days was provided in SI.

2.4.2. The effect of Gastrodin/PU NGCs on nerve regeneration

An experimental sciatic nerve defect injury animal model involved sixty rats. Rats were randomly divided into autograft, PU, 1%Gastrodin/

PU and 5%Gastrodin/PU groups. Surgeries were performed using an operating microscope under aseptic techniques (Fig. S2(A)). After anesthetizing, an incision was made in the gluteal muscle. The sciatic nerve in the right hind limb was exposed and a 10 mm segment of the nerve was removed. For autograft group, proximal and distal stumps of the nerve was repaired using the reversed autologous nerve segment using 8–0 absorbable sutures. For experimental groups, the NGCs of 12 mm were implanted between the proximal and distal stumps and sutured. Following, the muscle incision was sutured using 5–0 absorbable sutures and the skin was closed with 3–0 absorbable sutures. Postoperatively, every five animals were fed in a cage with free access to food and water. At 4, 12, 16 weeks, twenty animals were sacrificed and the implants with surrounding tissue were harvested (n = 5 per group) and fixed immediately in a cold buffered 4% paraformaldehyde solution. Additionally, sciatic function index, electrophysiological and histomorphometric analysis were performed at 16 weeks to estimate the efficiency of NGCs for nerve regeneration before the animals were sacrificed. Further details were showed in the SI.

2.5. Statistical analysis

The data were reported as the mean ± standard deviations (SD). One-way analysis of variance (ANOVA) was applied for statistical comparisons among groups more than two, and *t*-test was used for the statistical comparisons among two groups. All statistical analysis was performed in the software GraphPad Prism 8.0. The values of $p < 0.05$ were considered statistically significant.

3. Results

3.1. Preparation and characterization of Gastrodin/PU NGC

The schematic of Gastrodin/PU NGC is illustrated in Fig. 1A. The NGC had inner diameter of 1.28 mm and outer diameter of 2.8 mm (Fig. 1B (a, d)). The microstructure of cross-section (b, c) and longitudinal section (e, f) was viewed using SEM (Fig. 1B). The NGC displayed the well-distributed and interconnected pore structure with pore size from 10 to 60 μm, and there was no difference between PU and

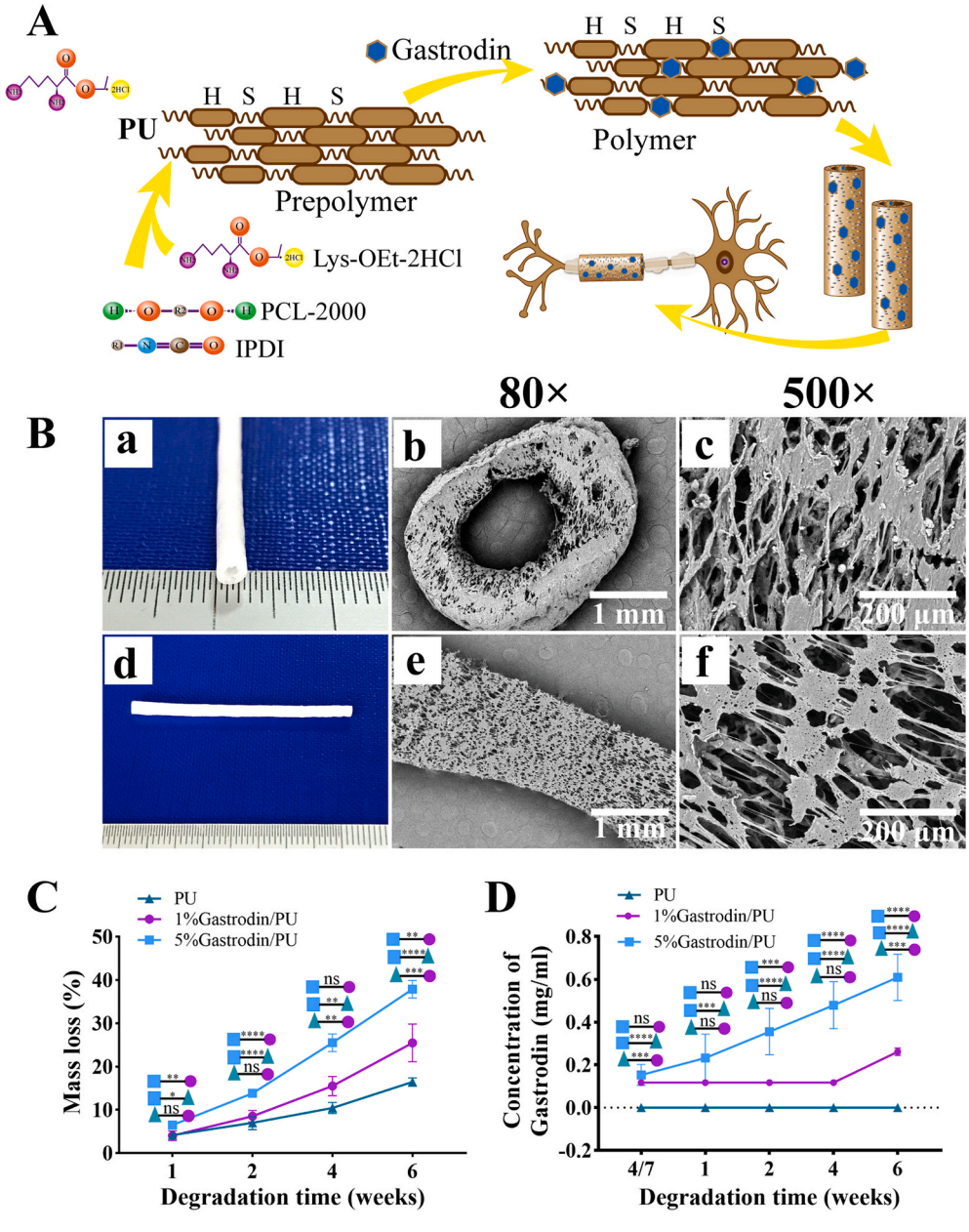

Fig. 1. Synthesis and characteristics of Gastrodin/PU NGCs. (A) Illustration of Gastrodin/PU NGCs preparation and their application for a peripheral nerve repair strategy. (B) Digital photos (a, d) and SEM images (b–c: cross-section; e–f: longitudinal section) of NGCs depicting interconnected pore structure. (C) Effect of Gastrodin on mass loss of NGCs against degradation time. (D) Gastrodin release profiles. Data are expressed as the mean ± SD (n = 5). *p < 0.05; **p < 0.01; ***p < 0.001; ****p < 0.0001.

Gastrodin/PU groups, consistent with our previous report [32].

The mass loss and Gastrodin release profile were quantified to evaluate their degradation properties. As shown in Fig. 1C, there was a significantly higher degradation rate for 5%Gastrodin/PU compared with 1%Gastrodin/PU group, while PU was slowest. The difference between groups became more evident as degradation time extended. Correspondingly, the Gastrodin was released from the 5%Gastrodin/PU in a controlled and sustained manner for 6 weeks with no evidence of an initial burst release, while obvious release in 1%Gastrodin/PU was only observed at 6th week (Fig. 1D).

3.2. The influence of Gastrodin/PU NGC on SCs behaviors

The peripheral nerve regeneration starts from the proliferation and migration of SCs, subsequently to support axonal outgrowth and myelinization. Meanwhile, SCs produce abundant trophic factors for axonal regeneration. Hence, to determine the supportiveness of Gastrodin/PU scaffolds for cell bioactivity, SCs were seeded onto the scaffolds. In Fig. 2A, B, the cell migration behaviors applied with Gastrodin/PU were significantly improved than that in other groups after 24 and 48 h, while the 5%Gastrodin/PU drove faster wound-healing rate. After 3 days culture, the cells covered the most of areas on these samples, and the cells on the internal wall of NGCs were more than the outer surface (Fig. 2C). These results suggested that scaffolds not only supported cell proliferation but also guided cell infiltration and spatial distribution. Interestingly, cytoskeleton of SCs in the 5%Gastrodin/PU was elongated, while the cells in the PU and 1%Gastrodin/PU groups were round. Live/Dead staining observed more spread cytoskeleton and nuclei of SCs in 5%Gastrodin/PU, and better growth and proliferation than others (Fig. S2). Meanwhile, a few dead cells (red) on PU and 1%Gastrodin/PU, but a markedly higher activity of cells on 5%Gastrodin/PU (green) were visible, confirmed well cytocompatibility in latter.

The effects of scaffolds on regulating SCs' myelination were investigated. Obviously, optical density of NGF was significantly elevated in the 5%Gastrodin/PU group on day 3 compared to those in the PU or 1% Gastrodin/PU treatment groups (Fig. 3A, B). The higher gene expression of GDNF and BDNF was also detected in 5%Gastrodin/PU than any other scaffolds, while NCAM, a promyelination marker and only expressed in immature SCs, was much lower, implying the onset of SCs myelination (Fig. 3C). Western blotting analysis results also showed that higher neurotrophic factors (EGR2, NGF, GDNF and BDNF) and lower NCAM protein levels on 5%Gastrodin/PU compared with that on other samples (Fig. 3D, E). These results demonstrated the benefits of optimum content of Gastrodin onto the PU scaffolds in the greatest extent of SCs myelination.

As a neuronal cell model, PC12 cells morphological differentiation was examined by adding the medium suspension from SCs culture with scaffolds (Fig. 4A). As shown in Fig. 4B, PC12 cells cultured with 5% Gastrodin/PU/SCs conditioned medium for 3 days exhibited longer neurite length than 1%Gastrodin/PU/SCs group or the culture with PU/

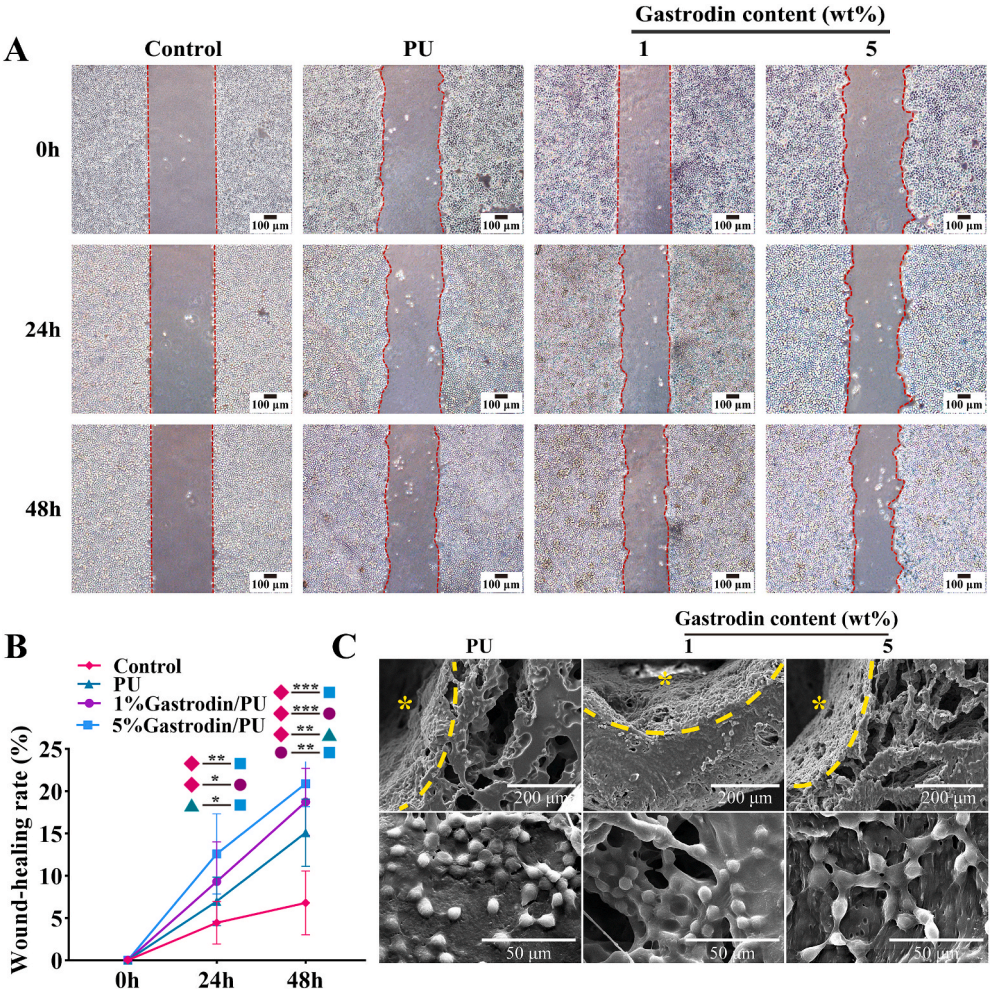

Fig. 2. The migration and proliferation of SCs on PU, 1%Gastrodin/PU, 5%Gastrodin/PU scaffolds at 3 days. (A) Cell migration in scratch assay. (B) Quantitative analysis of the migratory ability of SCs. (C) SEM images of SCs. * indicates internal surface of NGCs. Data are expressed as the mean ± SD (n = 5). *p < 0.05; **p < 0.01; ***p < 0.001.

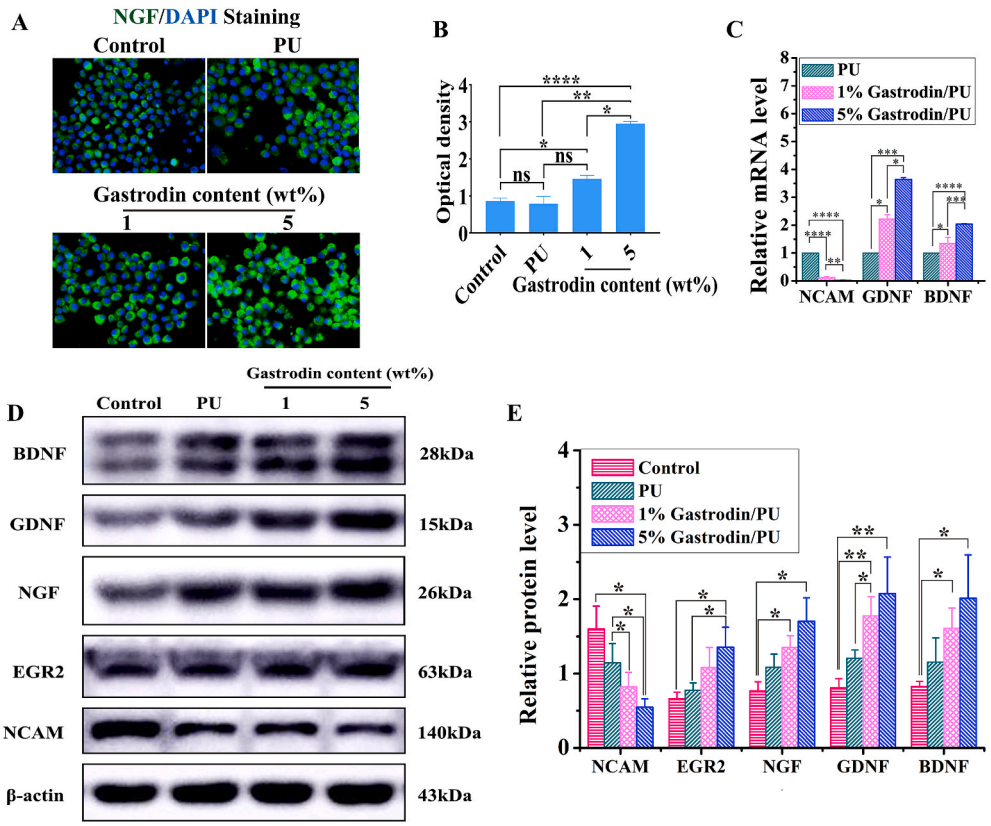

Fig. 3. The differentiation of SCs on PU, 1% Gastrodin/PU, 5%Gastrodin/PU scaffolds at 3 days. (A) NGF immunofluorescent images of SCs. (B) Quantitative analysis of the optical density from NGF staining. (C) Relative genes level of NCAM, GDNF and BDNF. (D) NCAM, EGR2, NGF, GDNF and BDNF protein expression of SCs measured by Western blotting and (E) the calculated corresponding protein levels. Data are expressed as the mean ± SD (n = 5). *p < 0.05; **p < 0.01; ***p < 0.001; ****p < 0.0001.

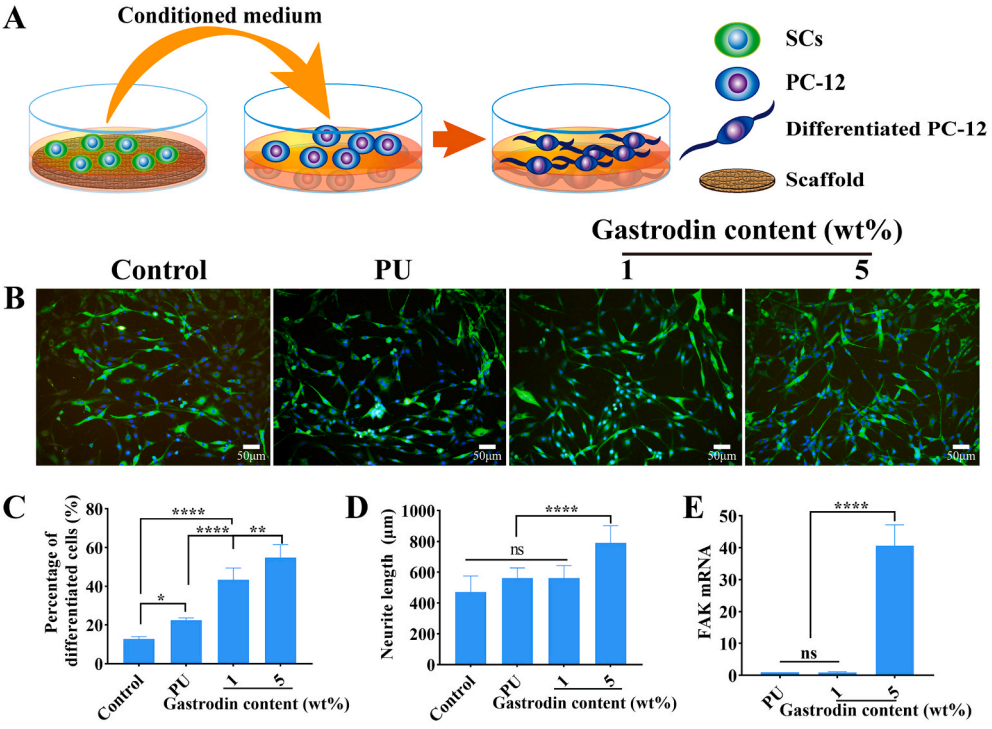

Fig. 4. PC12 cell differentiation incubated with scaffolds/SCs conditional medium after 3 days. (A) Schematic of indirect coculture of PC12 cells. (B) Staining cytoplasm (β-Tubulin-III, green) and nucleus (blue) of PC12 cells. Quantitative results of percentage of differentiated PC12 cells (C) and neurite length (D). (E) FAK mRNA levels. Data are expressed as the mean ± SD (n = 5). *p < 0.05; **p < 0.01; ****p < 0.0001. (For interpretation of the references to colour in this figure legend, the reader is referred to the Web version of this article.)

SCs conditioned medium. The average neurite length in PC12 cells further confirmed this observation. Similar results were drawn from the percentage of differentiated PC12 cells (Fig. 4C, D). Contrastly, higher FAK expression cultured with 5%Gastrodin/PU/SCs conditioned medium was obvious, indicating positive adhesion effects (Fig. 4E). These results illustrated inderectly that 5%Gastrodin/PU would promote neurotrophins secretion from SCs.

3.3. Anti-inflammatory response

The effect of physicochemical features of biomaterials on the release of inflammatory cytokines from macrophages *in vitro* was assessed. It was found that the Raw264.7 cells could spread well on the scaffolds (Fig. 5A). The cells incubated with Gastrodin/PU caused a decrease of pro-inflammatory cytokines, more pronounced for 5%Gastrodin/PU compared with 1%Gastrodin/PU showing significantly decreased iNOS and TNF-α gene levels (Fig. 5B). Lower amounts of TNF-α protein expression also exhibited in 5%Gastrodin/PU from Elisa assay (Fig. 5C). By contrast, the macrophage-PU interaction resulted in an inflammatory microenvironment, suggesting that Gastrodin loaded PU significantly attenuated inflammation.

After confirming that the Gastrodin-enriched microenvironment could trigger an anti-inflammatory response *in vitro*, the modulation on day 3, 7 and 14 after subcutaneous implantation were determined. Immunostaining of TNF-α was performed to delineate host response to the scaffolds (Fig. 5D). On day 3, optical density was apparently decreased following Gastrodin/PU treated compared to those in PU group. Subsequently, the expression of inflammatory protein decreased with the healing process over the 14 days. Masson (Fig. 5E) staining further showed that fibrous capsules surrounding the 5%Gastrodin/PU was much thinner compared to the 1%Gastrodin/PU and PU groups at 3 days. The thickness of fibrous capsules decreased with the prolongation of implant time, especially for 5%Gastrodin/PU, evidencing by the sequent decrease of the fibrous capsule thickness (Fig. 5F).

As expected, there was a notably higher proportion of vessels generation for 5%Gastrodin/PU than other groups (Fig. S3). The systemic effects of Gastrodin/PU were also assessed. Serum chemistry examinations revealed that 5%Gastrodin/PU exhibited only a little decrease in the number of creatinine during the 14 days after treatment (Table S3), and the toxicity was not found.

3.4. Gastrodin/PU NGC promotes sciatic nerve regeneration and remyelination in vivo

Macroscopic examination of grafted defects revealed that the defects were successfully re-bridged (Fig. S4(B)). Ammonia silver staining clearly showed longitudinal regenerated nerve fibers at 4, 12 and 16 weeks postoperatively, and the fibers formed persistently with time. It was observed that the nerve fibers were nearly regenerated completely through the entire scaffold except slight arrangement without rules. Both the autograft and 5%Gastrodin/PU presented aligned fibers along the conduit by the bunch. However, the fiber was a little bit regeneration as well as no regular arrangement through the PU and 1%Gastrodin/PU in Fig. 6.

The results of H&E staining in middle-section of the nerve implants depicted regenerative neuro-filaments. At 4 weeks, the nerve fibers in the autograft group were significantly denser than those in the scaffold groups. Obviously, a significant improvement in the regeneration of fibers was observed within 5%Gastrodin/PU group, as compared to 1% Gastrodin/PU and PU (Fig. 7A-D). At 12 weeks, the density of the nerve fibers in both the 5%Gastrodin/PU and 1%Gastrodin/PU groups were further enhanced, although could not be fully comparable to that in the autograft group, whereas the fiber density in the PU group was significantly lower (Fig. 7E-H). The difference was more pronounced at 16 weeks. Visibly, the 5%Gastrodin/PU had higher density of neuro-filaments than 1%Gastrodin/PU and PU groups. (Fig. 7I-L).

Microvessel formation within the regenerated nerve was specifically evaluated based on H&E staining (Fig. 7i-l) and immunofluorescent staining for CD31 (Fig. 7M-P) at 16 weeks. Newly formed microvessels were observed in Gastrodin/PU groups. Notably, 5%Gastrodin/PU showed higher microvessel density than 1%Gastrodin/PU. Furthermore, immunofluorescent staining for CD31, a marker of vascular endothelial cells, also revealed more microvessels in Gastrodin/PU groups.

Moreover, a sign of inflammation in PU group (Fig. 7B) at 4 weeks was observed, while the other defects were successfully re-bridged without signs of inflammation. Compared to PU, the Gastrodin/PU groups presented less fiber wrapping after implantation. No obvious

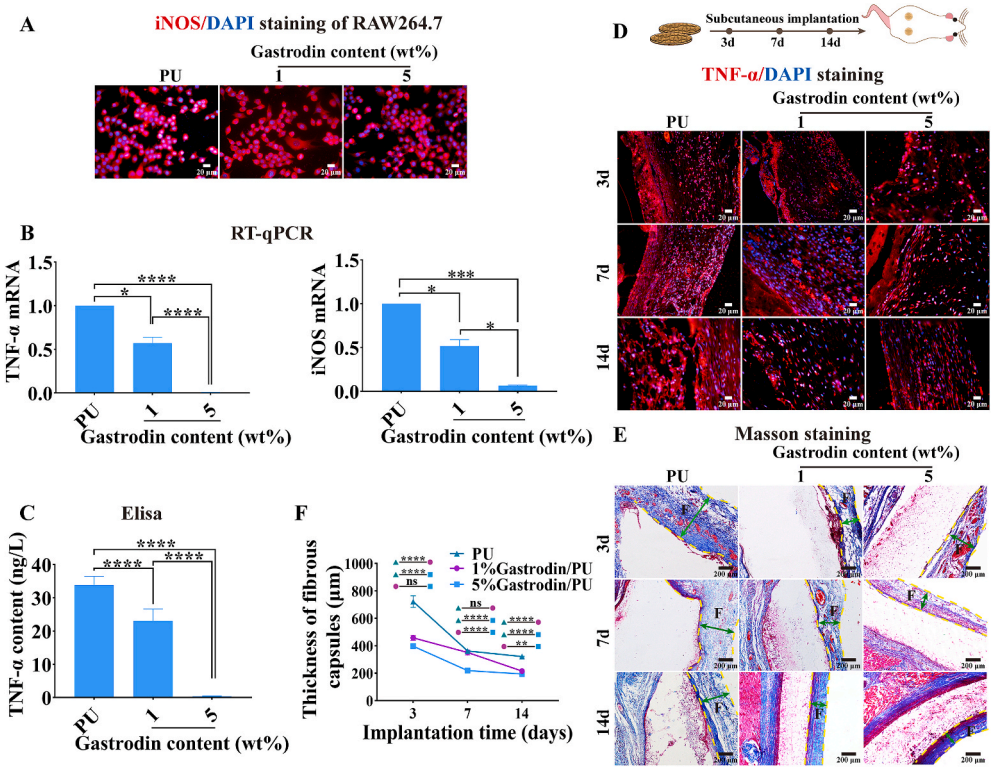

Fig. 5. Efficacy on anti-inflammatory properties of Gastrodin/PU scaffolds. (A–C) Scaffolds incubated with Raw264.7 cells for 3 days: (A) Staining cytoplasm (iNOS, red) and nucleus (blue) of cells; (B) RT-qPCR analysis; (C) The content of TNF-α protein. (D–F) Host response to the scaffolds following 14-day subcutaneous implantation: (D) Immunofluorescent (TNF-α) staining; (E) Masson staining; (F) Quantitative results of thickness of fibrous capsules from Masson staining. "F" denotes fibrous capsules; two-way green arrows mark the span of the fibrous capsule at the film-tissue interface. Data are expressed as the mean ± SD (n = 5). *p < 0.05; **p < 0.01; ***p < 0.001; ****p < 0.0001. (For interpretation of the references to colour in this figure legend, the reader is referred to the Web version of this article.)

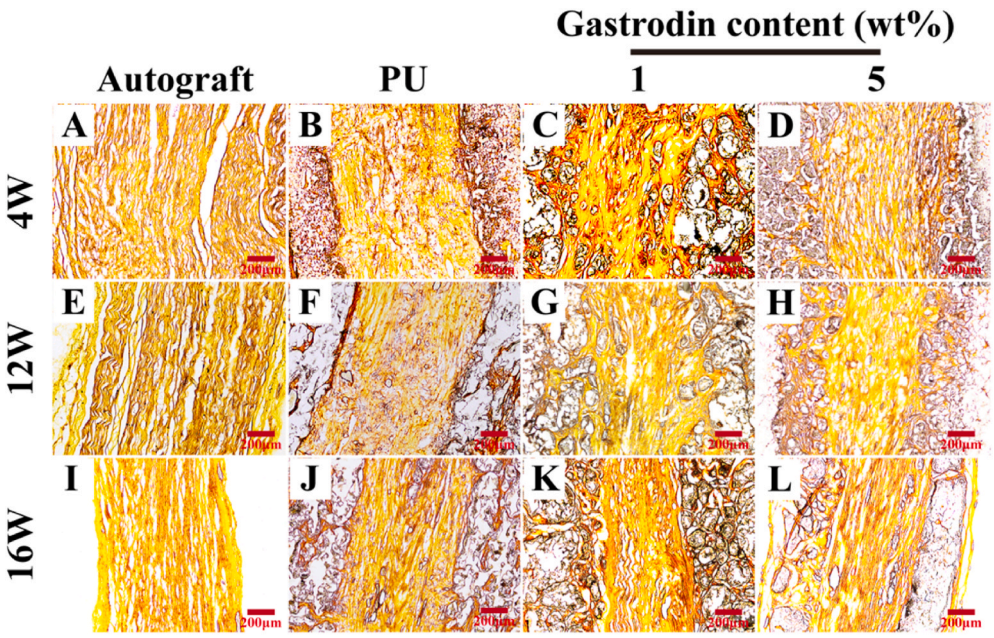

Fig. 6. Ammonia silver staining longitudinal section of the middle-regenerated nerve at 4 (A–D), 12 (E–H), 16 (I–L) weeks implantation: (A, E, I) Autograft; (B, F, J) PU; (C, G, K) 1%Gastrodin/PU; (D, H, L) 5%Gastrodin/PU.

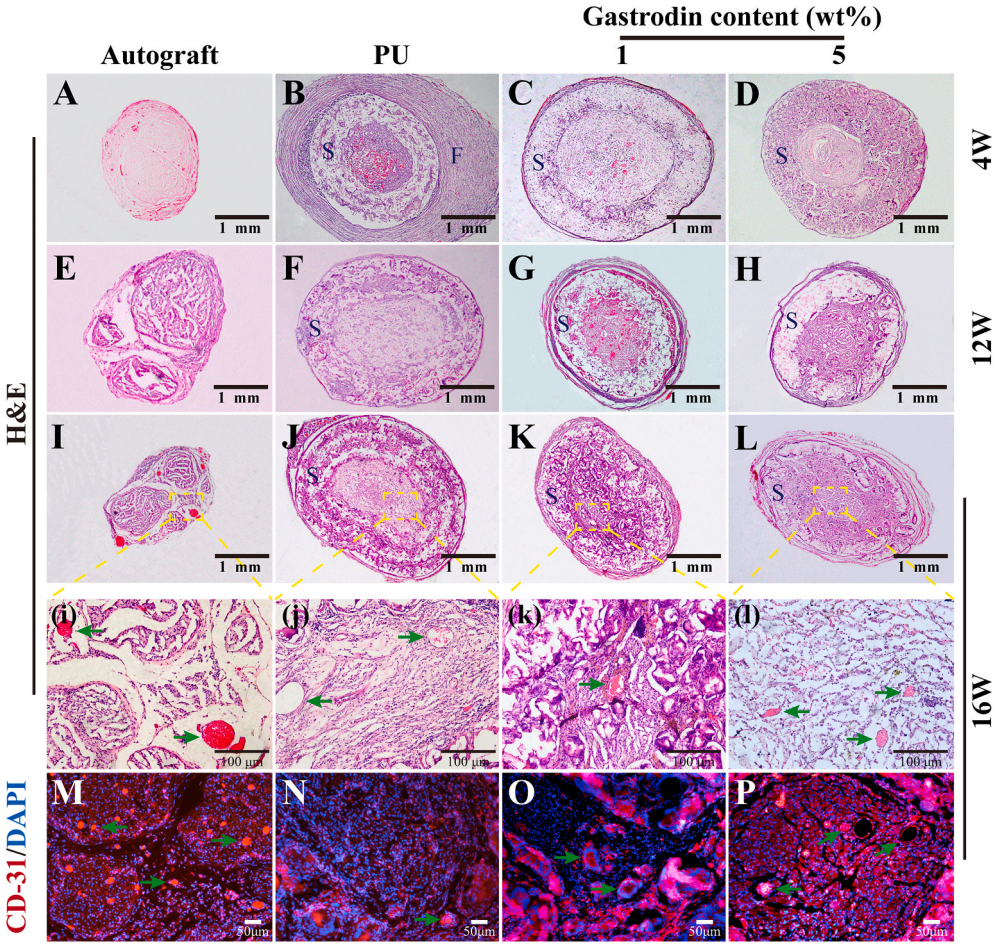

Fig. 7. Middle cross-section microstructure of the regenerated nerves. H&E stained at 4 (A–D), 12 (E–H), 16 (I–L) weeks and CD31 stained at 16 (M – P) weeks implantation: (A, E, I, M) Autograft; (B, F, J, N) PU; (C, G, K, O) 1%Gastrodin/PU; (D, H, L, P) 5%Gastrodin/PU. S - Scaffolds; F - Fibrous capsules; Green arrows indicate the microvessels. (For interpretation of the references to colour in this figure legend, the reader is referred to the Web version of this article.)

degradation occurred in the PU group over the entire period, and the conduits remained intact and rigid. In contrast, the Gastrodin/PU groups showed significant degradation, especially for 5%Gastrodin/PU, enlarged pore size and thinner tuber wall was observed at 16 weeks.

The regenerated nerve tissues were stained with immunofluorescent indicators NF-200 (expression of axon maturation markers) to demonstrate the nerve fibers within the regenerated nerve at 16 weeks. As shown in Fig. 8A, B, the positive expressions of the NF-200 were generated in these groups. The 5%Gastrodin/PU group was closest to autograft with more homogeneous axons compared with the PU and 1% Gastrodin/PU groups. Quantitative analysis results showed that the positive area in the 5%Gastrodin/PU and autograft groups were significantly more than the 1%Gastrodin/PU and PU groups. There was no significant difference between the 5%Gastrodin/PU and the autograft groups (Fig. 8D).

To further survey the recovery of regenerated nerve, β-Tubulin-III and the corresponding positive area were studied. β-Tubulin-III, as a marker protein of the microtubules formation of nerve regenerated axons, is primarily expressed in neurons and may be involved in neurogenesis and axon guidance and maintenance [39].The results of the images analysis showed that the microtubules have regenerated. The 1% Gastrodin/PU and PU groups showed minor nerve fiber growth. The 5% Gastrodin/PU group was found to have more sturdy and homogeneous microtubules compared with the PU and 1%Gastrodin/PU groups (Fig. S6), which were closest to the autograft group. Similar result was confirmed with the staining of NF-200.

The sub-microstructure and axonal regeneration myelin thickness of middle regenerated nerves were measured according to the TEM images. As shown in Fig. 8C, the thinnest myelin sheath and smallest diameter were observed in the PU group, while the thickness of regenerated axons in 5%Gastrodin/PU and 1%Gastrodin/PU groups were improved, but still lower than the autograft group. The statistical results also indicated that there was marked enhancement in the myelin thickness with increased loaded-Gastrodin content (Fig. 8E). It could indicate more regeneration of nerve fiber with myelin sheathes on 5%Gastrodin/PU group.

3.5. Gastrodin/PU NGC promotes function and electrical conduction recovery

After sciatic nerve injury, the denervated muscles begin to atrophy, leading to limb paralysis. By recording rat footprints, the degree of reinnervation functional recovery could be quantified. The walking track analysis in each group was conducted at 16 weeks postoperatively. As illustrated in Fig. 9A, photographs of the footprints indicated that the toes of the rats spread in the 5%Gastrodin/PU group were similar to that in the autograft and better than those in the PU and 1%Gastrodin/PU groups, indicating a recovery in motor function. The SFI was calculated to evaluate the functional recovery of the regenerated nerves (Fig. 9B). As the SFI value approached zero, the corresponding functional recovery was improved. The SFI value in the 5%Gastrodin/PU group was significantly higher than those in the PU and 1%Gastrodin/PU groups, while the autograft group showed the most evident improvement. These results suggested that the 5%Gastrodin/PU could significantly improve the functional recovery after sciatic nerve injury.

The recovery of nerve conduction was then evaluated by electrophysiological analysis. The parameter of CMAP, reflecting the number of nerve fibers innervating the target muscle, can offer a significant evidence for evaluation scaffolds' conducting function of peripheral nerve [40]. The typical CMAP curves of each group at 16 weeks after surgery was recorded, as depicted in Fig. 9C. Amplitude of CMAP, in the 5% Gastrodin/PU group was significantly better than those of 1%Gastrodin/PU and PU groups, closest to autograft group, but all of them were inferior to autograft (Fig. 9D), indicating the positive effects of loaded Gastrodin on restoring nerve conduction function.

The atrophy of gastrocnemius muscle resulted from dysfunction of the sciatic nerves was further evaluated. The gross images of the harvested muscles showed that sciatic nerve injury caused muscle atrophy of the injured site and the size of the muscle had not recovered to normal at 16 weeks (Fig. 9E). The Masson staining showed that much more regular and homogeneous muscular shape were observed in autograft and 5%Gastrodin/PU groups than those in 1%Gastrodin/PU and PU groups (Fig. 9F), and the later presented more marked muscular atrophy and adhesion. Similar results were further verified by the immunofluorescent staining of anti-laminin (Fig. 9G). Laminin, as an extracellular matrix glycoprotein, was used to measure further the shape of gastrocnemius bundle. The statistically average diameter of the muscle fiber in 5%Gastrodin/PU was larger than that of the fibers in PU and 1%Gastrodin/PU groups, yet smaller than that of the autograft (Fig. 9I). The wet weight ratios of gastrocnemius muscles (Fig. 9H) also indirectly confirmed muscle atrophy. The data in the 5%Gastrodin/PU group was significantly higher than that in 1%Gastrodin/PU and PU groups, although still lower than that in the autograft group. The attenuated reduction in muscle mass observed in 5%Gastrodin/PU group denoted a lessened degree of muscle denervation atrophy, suggesting enhanced neuro-regeneration.

4. Discussion

After peripheral nerve injury, SCs begin to proliferate and guide the regeneration of proximal axons. The supportiveness of NGCs for SCs biological behavior and bridging the proximal and distal nerve stumps is

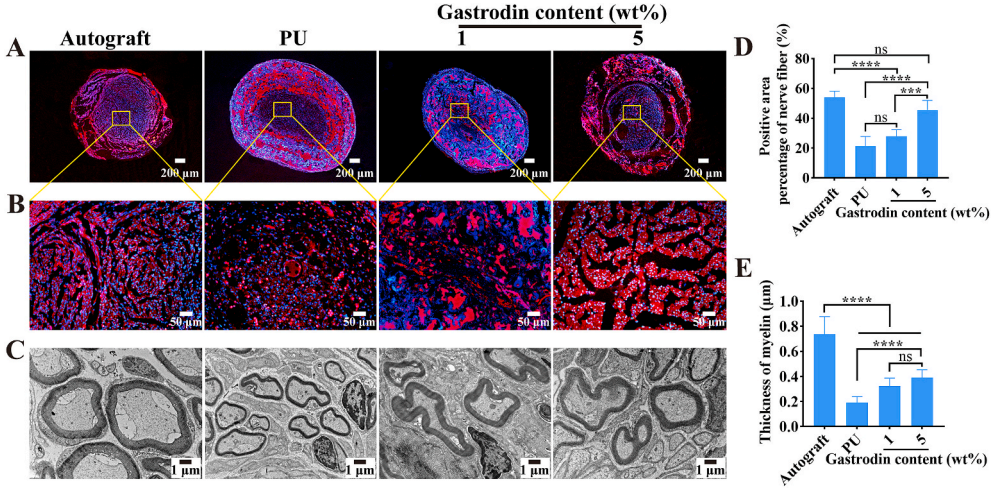

Fig. 8. Cross section immunofluorescent staining of regenerated nerves at the middle graft level for neurofilaments (A, B, NF-200, red) and counterstained with DAPI (blue) at 16 weeks: autograft, PU, 1%Gastrodin/PU and 5%Gastrodin/PU. Yellow square magnifications of immunostainings demonstrating nerve fascicle details and the contained regenerated axons. (C) TEM images of transverse sections of regenerated nerve fibers at 16 weeks. (D) Positive area percentage of nerve fiber from NF-200 staining. (E) The average regenerating myelin sheath thickness. Data are expressed as the mean ± SD (n = 5). **p < 0.01; ***p < 0.001; ****p < 0.0001. (For interpretation of the references to colour in this figure legend, the reader is referred to the Web version of this article.)

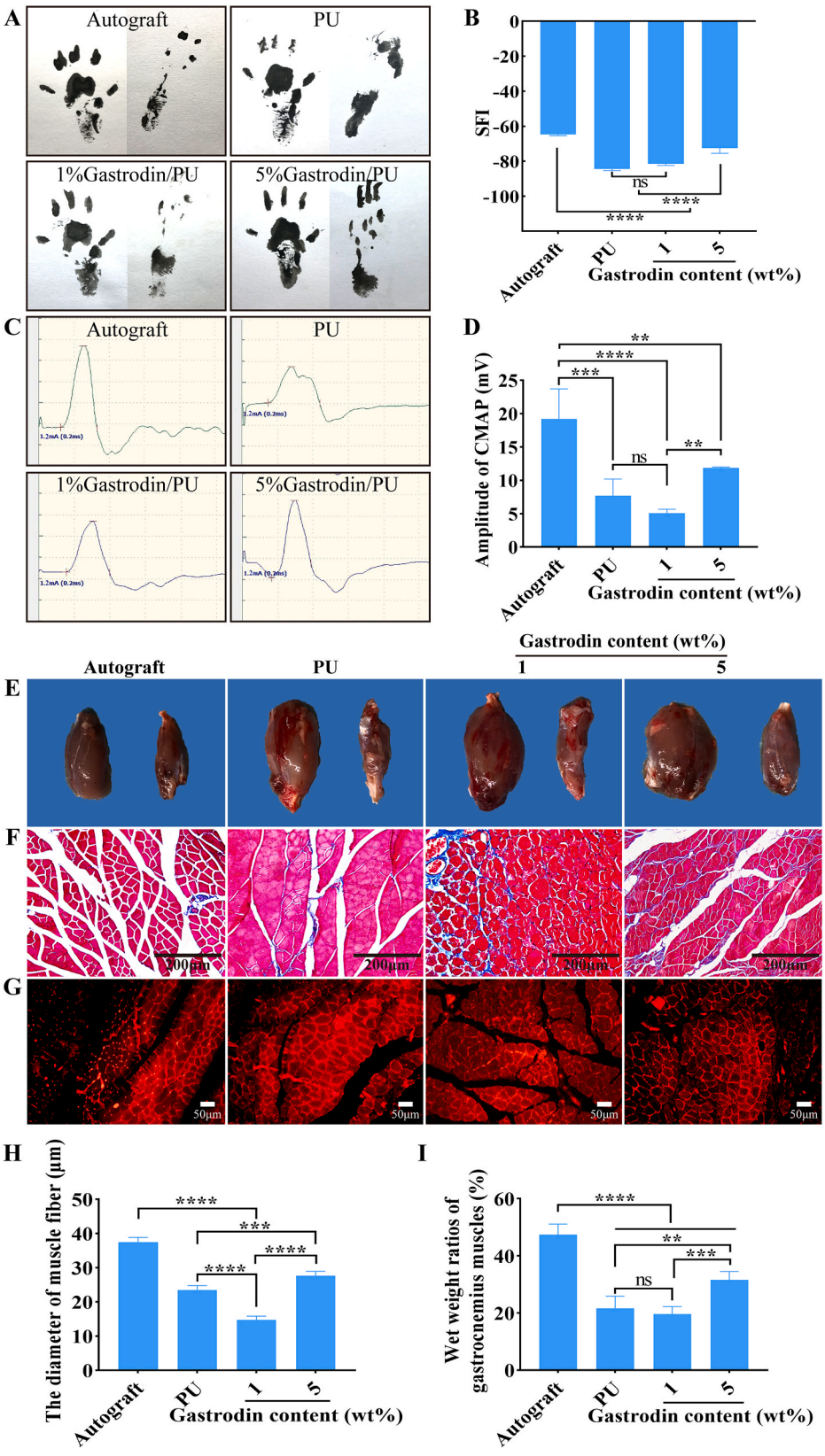

Fig. 9. Recovery of function and electrical conduction at 16 weeks postoperatively. (A) Representative images of left (normal) and right (injured) footprints. (B) Sciatic functional index (SFI). (C) The complex muscle action potential (CMAP). (D) Statistical analysis of CMAP amplitude in each group. (E) Representative images of gastrocnemius muscles. (F) Masson and (G) Anti-laminin immunofluorescent staining images of cross-sections of gastrocnemius muscles. (H) Statistical results of the wet weight ratios of gastrocnemius muscles. (I) Statistical analysis of the mean cross-sectional diameter of muscle fibers. Data are expressed as the mean ± SD (n = 5). *p < 0.05; **p < 0.01; ***p < 0.001; ****p < 0.0001.

critical nerve regeneration [33]. PUs with high flexibility and biocompatibility have been reported as NGCs to induce axonal extension or direct neurite outgrowth [6]. However, their neuro-regeneration effect should be enhanced for their clinical application. In this study, a functional Gastrodin was polymerized onto the PU conduits to provide a good microenvironment for minimizing the inflammatory responses and stimulating axonal regeneration.

The NGCs had pore interconnectivity and the pore size ranged from 10 to 60 μm (Fig. 1B). Generally, a pore size of 20–60 μm is optimal for maximum axon penetration and minimum axon misdirection [41].

Incorporation of Gastrodin into PU statistically augmented flexibility and elongation at break, which could provide a 3D framework for cell matrix deposition and nerve regeneration [36]. The hydrophilic Gastrodin also accelerated degradation by activating interaction between materials and degradation liquid (Fig. 1C). Correspondingly, sequential Gastrodin release would act as a promising pattern in the peripheral nerve tissue engineering. And 5%Gastrodin/PU realized long-term release of Gastrodin (Fig. 1D), which was likely to support neuroprotection and anti-inflammatory effect.

A great of many cells and cytokines are involved in the healing events to influence tissue repair after nerve injury. Previous studies have demonstrated positive effects of BDNF and GDNF on nerve repair and survival [42]. The elevated secretion may primarily account for the facilitated migration of axonal fibers and potentially involve in myelination [43]. During structural and functional recovery process, SCs also generate and release different cytokines, which in turn are involved in axonal activity, to establish a permissive growth microenvironment for guiding the nerve growth [44]. Ultimately, proliferative SCs transform to ensheath of immature axons [45]. NCAM is an indicator of SCs' promyelination. It is expressed only in immature SCs and decreases in SCs' myelination [46]. In the current design, introduction of Gastrodin to PUs could promote proliferation, migration and myelinating conversion of SCs with an elongated shape (Fig. 2). Elongated SCs are usually along their basal lamina to form bands of Büngner that support the guidance of outgrowing axons [47]. It was confirmed that Gastrodin/PU allowed SCs attachment, migration, cellular communication as well as cell division. Promoted cell proliferation might come from the increased hydrophilicity of 5%Gastrodin/PU, which has been confirmed in our previous reports [36], more affinity to encourage SCs adhesion. Coincidentally, De Luca et al. [48] reported a similar phenomenon that hydrophilic surface could achieve significant proliferation and attachment of SCs. Clearly, the enhanced cellular behaviors were also ascribed to the Gastrodin released from PU, maximally accelerating SCs infiltration into the luminal surfaces of NGCs, favoring guided axon ingrowth and myelination. The combination with interconnected pores of tube wall in NGCs was even more crucial for *in vivo* implantation, which assured a sufficient supply of nutrition and appropriate permeability for oxygen and metabolite to ingrowth nerve prior to the establishment of functional neovasculature. Additively, culture of SCs on 5% Gastrodin/PU showed reduced NCAM level for 3 days, indicating elevated myelinating capacity and neurotrophin secretion (Fig. 3). Consistent with the findings that myelinating SCs increased neurotrophic factors expression while reducing NCAM [49]. Significantly promoted secretion of EGR2, NGF, BDNF and GDNF was measured on 5%Gastrodin/PU compared to 1%Gastrodin/PU, which were able to promote PC12 differentiation (Fig. 4), suggesting the regulatory role of 5%Gastrodin/PU in maturation of SCs. The myelinating SCs usually up-regulate myelin markers and release neurotrophins, relevant to peripheral nerve regeneration.

As a foreign body, implanted NGCs inevitably trigger an inflammatory response that manipulates the regeneration process of peripheral nervous damage [50]. Inferior nerve implants usually appear a long period of chronic inflammation, resulting in fibrotic encapsulation of the materials. Many studies have showed that fibrotic response in pathological conditions impaired proper function of organ [51]. Hence, it is necessary to endow implant with anti-inflammatory function. Our group previously reported that Gastrodin mediated anti-inflammatory effects in activated microglia by modulating the Wnt/β-catenin, down-regulating expression of iNOS, TNF-α and NO levels [52]. Subsequent study further reported that localized release of Gastrodin based polymer significantly reduced TNF-α and IL-1β level, indicating an anti-inflammatory response [37]. And we expect the Gastrodin/PU NGCs to have similar influences in this study. The Gastrodin/PU exhibited a high effect on anti-inflammation according to the results of remarkedly down-regulating iNOS and TNF-α expression in RAW264.7 cells, which was particularly obvious in 5%Gastrodin/PU (Fig. 5A-C). Consistent with *in vitro* results, there was significant improvement on inflammatory microenvironment *in vivo* using Gastrodin/PU scaffolds. Subcutaneous implantation revealed a reduction of fibrous capsule (Fig. 5E) and low expression of TNF-α (Fig. 5D) around Gastrodin/PU. Only thick fibrous capsule was observed around the PU (Fig. 7B) in the nerve implantation after 4 weeks, accompanied by the disappearance of the inflammatory response in subsequent time-points. The inhibition of inflammatory development at the site of nerve damage showed a positive feedback effect on nerve regeneration [53]. Neumann et al. [54] reported increased neurite outgrowth when inflammatory factors like TNF-α secretion were inhibited.

The dual function of SCs myelination and anti-inflammatory promotion contributes to create a microenvironment conducive for axonal regeneration and tissue repair [55]. After peripheral nerves are injured, SCs start proliferation and migration into the injury site, interact with axons to form the myelin sheath during their growth and maturation, resulting in the subsequent myelination of regenerated nerve fibers [56]. More importantly, myelinated fibers can deliver signals to the target muscle [57], and the presence of myelinated axons provides the structural basis for improvements in nerve conduction and functional recovery [58].The ultra-structure of the regenerated nerve tissues showed that after 16 weeks, myelin sheath thickness was significantly enhanced when treated with Gastrodin/PU (Fig. 8C, E). From morphological evaluation of ammonia silver, H&E, NF-200 and β-Tubulin-III staining results after 4, 12, 16 weeks, it was found that the regenerated nerve fibers in the 5%Gastrodin/PU group had more dense and regular morphological features similar to the nerve tissue morphology of autograft than that in 1%Gastrodin/PU and PU groups, and the enhancement was persistent with time (Figs. 6–8 and S5-S6), which explained why the 5%Gastrodin/PU group had more spread footprint areas (Fig. 9A). Of note was that 5%Gastrodin/PU group achieved a comparable amount of neo-microvessels to autografts (Fig. 7L, P), which in turn resulted in comparable nerve regeneration and function recovery of the regenerated nerves between 5%Gastrodin/PU group and autografts. The significant neo-microvessels regeneration treated with Gastrodin/PU was also visible in the subcutaneous implantation (Fig. S3), which has been evidenced by our previous Gastrodin modified vascular scaffolds experiments [37]. In fact, competent microvascular network reconstruction guarantees tissue regeneration and restoration of physiological functions, as it permits a sufficient nutrient supply [59]. Further, the walking track analysis (SFI, Fig. 9 (A, B) and electrophysiology (CMAP, Fig. 9 (C, D) after 16 weeks showed that Gastrodin/PU had less loss of nerve function than PU, indicating that the Gastrodin modified PU improved the nerve functional restoration. This difference might reflect the fast degradation of scaffolds accompanied by the release of Gastrodin (Fig. 1D) leading to up-regulating neurotrophins supply. When the Gastrodin release was optimized, 5%Gastrodin/PU achieved better effect. It is well known that adequate neurotrophins treatment had therapeutic index in reduced atrophy of gastrocnemius [40]. Masson and anti-laminin staining results indicated a reduction in the extent of denervation muscular atrophy with the 5%Gastrodin/PU, being closer to that in autograft and better than that in the 1%Gastrodin/PU and PU groups (Fig. 9H and Fig. S7).

Altogether, the promotion effect of Gastrodin/PU for peripheral nerve regeneration has realized through regulation of neuroprotection-related cytokines and favorable biological properties to create an appropriate microenvironment for nerve regeneration. Current 5%Gastrodin/PU offers compelling evidence of directing SCs biological function, inducing nerve fibers formation and angiogenesis, and eventually contributing to nerve functional recovery (Fig. 10). Although the role of Gastrodin on nerve protection has been studied extensively, Gastrodin released from biomaterials is still in primary stage, and precise mechanism of Gastrodin/PU on nerve repair needs our further exploration. In addition, PU NGCs modified with 5 wt% Gastrodin have achieved positive effect on peripheral nerve repair in SD rat, however, the systematized Gastrodin release profile and its dynamic manipulation on nerve

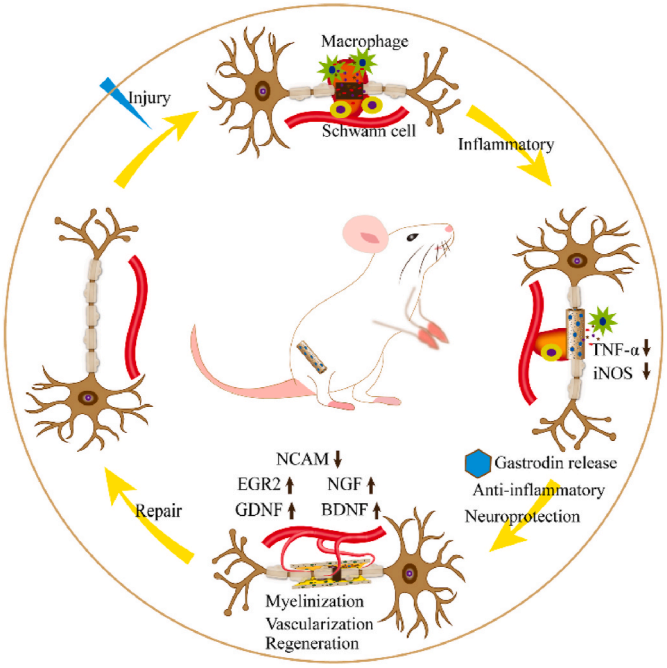

Fig. 10. The mechanism of functional Gastrodin/PU NGC to accelerate peripheral nerve repair.

regeneration remains a challenge. Thus, a deep investigation may focus on the detailed mechanism of Gastrodin/PU for peripheral nerve regeneration, promoting its biomedical applications.

5. Conclusion

A functional Gastrodin/PU NGC is used to bridge nerve stumps. Gastrodin is effectively bonded to the scaffolds that undergoes a well-controlled release. Compared to the PU and 1%Gastrodin/PU scaffolds, 5%Gastrodin/PU scaffold significantly promotes SCs proliferation, migration, myelination, and up-regulates trophic factors expression; proved to promote the differentiation of PC12 cell. The release of Gastrodin reduces the proinflammatory cytokines iNOS and TNF-α levels, and the fibrous capsule of Gastrodin/PU is few in implantation. Through the evaluation of morphological and functional recovery of regenerated nerve, it is found that 5%Gastrodin/PU can successfully repair a 10 mm sciatic nerve defect and exhibit a similar healing capacity to autograft. The 5%Gastrodin/PU has effective enhancement on the numbers of axons and microvessels of regenerated tissue, followed by axonal remyelination and functionalization. In addition to the fast recovery rate, the ability to have regenerated tissue with normal morphology makes 5%Gastrodin/PU to be a powerful candidate to repair the peripheral nerve damages.

CRediT authorship contribution statement

Hongcai Yang: Investigation, Formal analysis, Visualization. **Qing Li:** Investigation, Data curation. **Limei Li:** Conceptualization, Writing – original draft. **Shaochun Chen:** Formal analysis. **Yu Zhao:** Visualization. **Yingrui Hu:** Investigation. **Lu wang:** Formal analysis. **Xiaoqian Lan:** Formal analysis. **Lianmei Zhong:** Resources, Supervision. **Di Lu:** Resources, Conceptualization, Writing – review & editing.

Declaration of competing interest

The authors declare that they have no known competing financial interests or personal relationships that could have appeared to influence the work reported in this paper.

Acknowledgements

This research was supported by the National Natural Science Foundation of China (81960251/81460210/81860326), the Department of Science and Technology of Yunnan Province of China (2019ZF011-2/2017FF117(-062)/2018IA048/2018FE001(-029)/2018FE001(-024)), Scientific Research Fund of Yunnan Provincial Education Commission (2021J0229), and the 100 Talents Program of Kunming Medical University (Limei Li).

Appendix A. Supplementary data

Supplementary data to this article can be found online at https://doi.org/10.1016/j.bioactmat.2021.06.020.

References

[1] K. Dalamagkas, M. Tsintou, A. Seifalian, Advances in peripheral nervous system regenerative therapeutic strategies: a biomaterials approach, Mater. Sci. Eng. C 65 (2016) 425–432, https://doi.org/10.1016/j.msec.2016.04.048.
[2] S. Geuna, I. Papalia, G. Ronchi, F.S. d'Alcontres, K. Natsis, N.A. Papadopulos, M. R. Colonna, The reasons for end-to-side coaptation: how does lateral axon sprouting work? Neural Regen Res 12 (4) (2017) 529–533, https://doi.org/10.4103/1673-5374.205081.
[3] T. Kornfeld, P.M. Vogt, C. Radtke, Nerve grafting for peripheral nerve injuries with extended defect sizes, Wien Med. Wochenschr. 169 (9–10) (2019) 240–251, https://doi.org/10.1007/s10354-018-0675-6.
[4] A.X. Sun, T.A. Prest, J.R. Fowler, R.M. Brick, K.M. Gloss, X. Li, M. DeHart, H. Shen, G. Yang, B.N. Brown, P.G. Alexander, R.S. Tuan, Conduits harnessing spatially controlled cell-secreted neurotrophic factors improve peripheral nerve regeneration, Biomaterials 203 (2019) 86–95, https://doi.org/10.1016/j.biomaterials.2019.01.038.
[5] M. Sarker, S. Naghieh, A. McInnes, D. Schreyer, X. Chen, Strategic design and fabrication of nerve guidance conduits for peripheral nerve regeneration, Biotechnol. J. 13 (2018), 1700635, https://doi.org/10.1002/biot.201700635.
[6] Y. Niu, K.C. Chen, T. He, W. Yu, S. Huang, K. Xu, Scaffolds from block polyurethanes based on poly(ϵ-caprolactone) (PCL) and poly(ethylene glycol) (PEG) for peripheral nerve regeneration, Biomaterials 35 (14) (2014) 4266–4277, https://doi.org/10.1016/j.biomaterials.2014.02.013.
[7] L. Wang, M.T. Sanford, Z. Xin, G. Lin, T.F. Lue, Role of Schwann cells in the regeneration of penile and peripheral nerves, Asian J. Androl. 17 (5) (2015) 776–782, https://doi.org/10.4103/1008-682X.154306.
[8] K.R. Jessen, R. Mirsky, A.C. Lloyd, Schwann cells: development and role in nerve repair, Cold Spring Harb Perspect Biol 7 (7) (2015), https://doi.org/10.1101/cshperspect.a020487 a020487-a020487.
[9] I. Martin, T.D. Nguyen, V. Krell, J.F.W. Greiner, J. Müller, S. Hauser, P. Heimann, D. Widera, Generation of Schwann cell-derived multipotent neurospheres isolated from intact sciatic nerve, Stem Cell Reviews and Reports 8 (4) (2012) 1178–1187, https://doi.org/10.1007/s12015-012-9387-2.
[10] L. Klimaschewski, B. Hausott, D.N. Angelov, Chapter six - the pros and cons of growth factors and cytokines in peripheral axon regeneration, in: S. Geuna, I. Perroteau, P. Tos, B. Battiston (Eds.), International Review of Neurobiology, vol. 108, Academic Press, 2013, pp. 137–171, https://doi.org/10.1016/B978-0-12-410499-0.00006-X.
[11] C. Cunha, S. Panseri, S. Antonini, Emerging nanotechnology approaches in tissue engineering for peripheral nerve regeneration, Nanomed. Nanotechnol. Biol. Med. 7 (1) (2011) 50–59, https://doi.org/10.1016/j.nano.2010.07.004.
[12] R. Li, D. Li, C. Wu, L. Ye, Y. Wu, Y. Yuan, S. Yang, Y. Mao, T. Jiang, Y. Li, J. Wang, H. Zhang, X. Li, J. Xiao, Nerve growth factor activates autophagy in Schwann cells to enhance myelin debris clearance and to expedite nerve regeneration, Theranostics 10 (2020) 1649–1677, https://doi.org/10.7150/thno.40919.
[13] C. Webber, K. Christie, C. Cheng, J. Martinez, B. Singh, V. Singh, D. Thomas, D. Zochodne, Schwann cells direct peripheral nerve regeneration through the netrin-1 receptors, DCC and Unc5H2, Glia 59 (2011) 1503–1517, https://doi.org/10.1002/glia.21194.
[14] J. Chen, S. Ren, D. Duscher, Y. Kang, Y. Liu, C. Wang, M. Yuan, G. Guo, H. Xiong, P. Zhan, Y. Wang, H.-G. Machens, Z. Chen, Exosomes from human adipose-derived stem cells promote sciatic nerve regeneration via optimizing Schwann cell function, J. Cell. Physiol. 234 (2019), https://doi.org/10.1002/jcp.28873.
[15] L.E. Kokai, A.M. Ghaznavi, K.G. Marra, Incorporation of double-walled microspheres into polymer nerve guides for the sustained delivery of glial cell line-derived neurotrophic factor, Biomaterials 31 (8) (2010) 2313–2322, https://doi.org/10.1016/j.biomaterials.2009.11.075.
[16] G. Lin, H. Zhang, F. Sun, Z. Lu, A. Reed-Maldonado, Y.-C. Lee, G. Wang, L. Banie, T. F. Lue, Brain-derived neurotrophic factor promotes nerve regeneration by activating the JAK/STAT pathway in Schwann cells, Transl. Androl. Urol. 5 (2016) 167–175, https://doi.org/10.21037/tau.2016.02.03.
[17] B. Wang, J. Yuan, X. Chen, J. Xu, Y. Li, P. Dong, Functional regeneration of the transected recurrent laryngeal nerve using a collagen scaffold loaded with laminin and laminin-binding BDNF and GDNF, Sci. Rep. 6 (2016) 32292, https://doi.org/10.1038/srep32292.

[18] M. Rosa, A. Sharma, S. Mallapragada, D. Sakaguchi, Transdifferentiation of brain-derived neurotrophic factor (BDNF)-secreting mesenchymal stem cells significantly enhance BDNF secretion and Schwann cell marker proteins, J. Biosci. Bioeng. 124 (2017), https://doi.org/10.1016/j.jbiosc.2017.05.014.

[19] A. Donsante, J. Xue, K. Poth, N. Hardcastle, B. Diniz, D. O'Connor, Y. Xia, N. Boulis, Controlling the release of neurotrophin-3 and chondroitinase ABC enhances the efficacy of nerve guidance conduits, Advanced Healthcare Materials 9 (2020), https://doi.org/10.1002/adhm.202000200.

[20] J. Lu, X. Yan, X. Sun, X. Shen, H. Yin, C. Wang, Y. Liu, C. Lu, H. Fu, S. Yang, y. Wang, X. Sun, L. Zhao, S. Lu, A. Mikos, J. Peng, X. Wang, Synergistic effects of dual-presenting VEGF- and BDNF-mimetic peptide epitopes from self-assembling peptide hydrogels on peripheral nerve regeneration, Nanoscale 11 (2019), https://doi.org/10.1039/C9NR04521J.

[21] C. Wang, Y. Jia, W. Yang, C. Zhang, K. Zhang, Y. Chai, Silk fibroin enhances peripheral nerve regeneration by improving vascularization within nerve conduits, J. Biomed. Mater. Res. 106 (7) (2018) 2070–2077, https://doi.org/10.1002/jbm.a.36390.

[22] G. Li, Q. Xiao, L. Zhang, Y. Zhao, Y. Yang, Nerve growth factor loaded heparin/chitosan scaffolds for accelerating peripheral nerve regeneration, Carbohydr. Polym. 171 (2017) 39–49, https://doi.org/10.1016/j.carbpol.2017.05.006.

[23] L. Li, J. Li, Q. Zou, Y. Zuo, B. Cai, Y. Li, Enhanced bone tissue regeneration of a biomimetic cellular scaffold with co-cultured MSCs-derived osteogenic and angiogenic cells, Cell Prolif 52 (2019), https://doi.org/10.1111/cpr.12658.

[24] A. Janse van Rensburg, N.H. Davies, A. Oosthuysen, C. Chokoza, P. Zilla, D. Bezuidenhout, Improved vascularization of porous scaffolds through growth factor delivery from heparinized polyethylene glycol hydrogels, Acta Biomater. 49 (2017) 89–100, https://doi.org/10.1016/j.actbio.2016.11.036.

[25] Z. Bin, Z. Zhihu, M. Jianxiong, M. Xinlong, Repairing peripheral nerve defects with revascularized tissue-engineered nerve based on a VEGF-heparin sustained release system, Journal of Tissue Engineering and Regenerative Medicine 14 (2020), https://doi.org/10.1002/term.3048.

[26] C. Lu, Y. Wang, S. Yang, C. Wang, X. Sun, J. Lu, H. Yin, W. Jiang, H. Meng, F. Rao, X. Wang, J. Peng, Bioactive self-assembling peptide hydrogels functionalized with brain-derived neurotrophic factor and nerve growth factor mimicking peptides synergistically promote peripheral nerve regeneration, ACS Biomater. Sci. Eng. 4 (8) (2018) 2994–3005, https://doi.org/10.1021/acsbiomaterials.8b00536.

[27] Y.-S. Joo, J.-R. Cha, M.-S. Gong, Biodegradable shape-memory polymers using polycaprolactone and isosorbide based polyurethane blends, Mater. Sci. Eng. C 91 (2018) 426–435, https://doi.org/10.1016/j.msec.2018.05.063.

[28] M. Caillaud, B. Chantemargue, L. Richard, L. Vignaud, F. Favreau, P.-A. Faye, P. Vignoles, F. Sturtz, P. Trouillas, J.-M. Vallat, A. Desmoulière, F. Billet, Local low dose curcumin treatment improves functional recovery and remyelination in a rat model of sciatic nerve crush through inhibition of oxidative stress, Neuropharmacology 139 (2018) 98–116, https://doi.org/10.1016/j.neuropharm.2018.07.001.

[29] E.F. Lim, V. Hoghooghi, K.M. Hagen, K. Kapoor, A. Frederick, T.M. Finlay, S. S. Ousman, Presence and activation of pro-inflammatory macrophages are associated with CRYAB expression in vitro and after peripheral nerve injury, J. Neuroinflammation 18 (1) (2021) 82, https://doi.org/10.1186/s12974-021-02108-z.

[30] J.R. Potas, F. Haque, F.L. Maclean, D.R. Nisbet, Interleukin-10 conjugated electrospun polycaprolactone (PCL) nanofibre scaffolds for promoting alternatively activated (M2) macrophages around the peripheral nerve in vivo, J. Immunol. Methods 420 (2015) 38–49, https://doi.org/10.1016/j.jim.2015.03.013.

[31] Z. Peng, S. Wang, G. Chen, M. cai, R. Liu, J. Deng, J. Liu, T. Zhang, Q. Tan, C. Hai, Gastrodin alleviates cerebral ischemic damage in mice by improving anti-oxidant and anti-inflammation activities and inhibiting apoptosis pathway, Neurochem. Res. 40 (4) (2015) 661–673, https://doi.org/10.1007/s11064-015-1513-5.

[32] Y. Yao, E.A. Ling, D. Lu, Microglia mediated neuroinflammation - signaling regulation and therapeutic considerations with special reference to some natural compounds, Histol. Histopathol. 35 (11) (2020) 1229–1250, https://doi.org/10.14670/HH-18-239.

[33] R. Zhang, Z. Peng, H. Wang, F. Xue, Y. Chen, Y. Wang, H. Wang, Q. Tan, Gastrodin ameliorates depressive-like behaviors and up-regulates the expression of BDNF in the Hippocampus and hippocampal-derived astrocyte of rats, Neurochem. Res. 39 (1) (2014) 172–179, https://doi.org/10.1007/s11064-013-1203-0.

[34] M.R. de Oliveira, F.B. Brasil, C.R. Fürstenau, Nrf2 mediates the anti-apoptotic and anti-inflammatory effects induced by Gastrodin in hydrogen peroxide–treated SH-SY5Y cells, J. Mol. Neurosci. 69 (1) (2019) 115–122, https://doi.org/10.1007/s12031-019-01339-3.

[35] H. Zhang, M. Liu, X. Ji, C. Jiang, Z. Li, B. OuYang, Gastrodin combined with rhynchophylline inhibits cerebral ischaemia-induced inflammasome activation via upregulating miR-21–5p and miR-331–5p, Life Sci. 239 (2019), 116935, https://doi.org/10.1016/j.lfs.2019.116935.

[36] Q. Li, L. Li, M. Yu, M. Zheng, Y. Li, J. Yang, M. Dai, L. Zhong, L. Sun, D. Lu, Elastomeric polyurethane porous film functionalized with Gastrodin for peripheral nerve regeneration, J. Biomed. Mater. Res. 108 (2020), https://doi.org/10.1002/jbm.a.36937.

[37] M. Zheng, J. Guo, Q. Li, J. Yang, Y. Han, H. Yang, M. Yu, L. Zhong, D. Lu, L. Li, L. Sun, Syntheses and characterization of anti-thrombotic and anti-oxidative Gastrodin-modified polyurethane for vascular tissue engineering, Bioact Mater 6 (2) (2021) 404–419, https://doi.org/10.1016/j.bioactmat.2020.08.008.

[38] X. Niu, R. Qin, Y. Zhao, L. Han, J. Lu, C. Lv, Simultaneous determination of 19 constituents in Cimicifugae Rhizoma by HPLC-DAD and screening for antioxidants through DPPH free radical scavenging assay, Biomed. Chromatogr. 33 (2019), https://doi.org/10.1002/bmc.4624.

[39] H. Huang, T. Yang, Q. Shao, T. Majumder, K. Mell, G. Liu, Human TUBB3 mutations disrupt netrin attractive signaling, Neuroscience 374 (2018) 155–171, https://doi.org/10.1016/j.neuroscience.2018.01.046.

[40] M. Jiang, X. Zhuge, Y. Yang, X. Gu, F. Ding, The promotion of peripheral nerve regeneration by chitooligosaccharides in the rat nerve crush injury model, Neurosci. Lett. 454 (3) (2009) 239–243, https://doi.org/10.1016/j.neulet.2009.03.042.

[41] R. Sridharan, R.B. Reilly, C.T. Buckley, Decellularized grafts with axially aligned channels for peripheral nerve regeneration, Journal of the Mechanical Behavior of Biomedical Materials 41 (2015) 124–135, https://doi.org/10.1016/j.jmbbm.2014.10.002.

[42] K. Uchida, H. Baba, Y. Maezawa, S. Furukawa, N. Furusawa, S. Imura, Histological investigation of spinal cord lesions in the spinal hyperostotic mouse (twy/twy): morphological changes in anterior horn cells and immunoreactivity to neurotropic factors, J. Neurol. 245 (12) (1998) 781–793, https://doi.org/10.1007/s004150050287.

[43] S.P. Frostick, Q. Yin, G.J. Kemp, Schwann cells, neurotrophic factors, and peripheral nerve regeneration, Microsurgery 18 (7) (1998) 397–405. https://doi.org/10.1002/(SICI)1098-2752(1998)18:7<397::AID-MICR2>3.0.CO;2-F.

[44] C. Ide, Peripheral nerve regeneration, Neurosci. Res. 25 (1996) 101–121, https://doi.org/10.1016/0168-0102(96)01042-5.

[45] K. Jessen, R. Mirsky, A. Lloyd, Schwann cells: development and role in nerve repair, Cold Spring Harb Perspect Biol 7 (2015), https://doi.org/10.1101/cshperspect.a020487.

[46] S. Yang, C. Wang, J. Zhu, C. Lu, H. Li, F. Chen, J. Lu, Z. Zhang, X. Yan, H. Zhao, X. Sun, L. Zhao, J. Liang, y. Wang, J. Peng, X. Wang, Self-assembling peptide hydrogels functionalized with LN- and BDNF- mimicking epitopes synergistically enhance peripheral nerve regeneration, Theranostics 10 (2020) 8227–8249, https://doi.org/10.7150/thno.44276.

[47] G. Nocera, C. Jacob, Mechanisms of Schwann cell plasticity involved in peripheral nerve repair after injury, Cell. Mol. Life Sci. 77 (20) (2020) 3977–3989, https://doi.org/10.1007/s00018-020-03516-9.

[48] A.C. De Luca, G. Terenghi, S. Downes, Chemical surface modification of poly-ε-caprolactone improves Schwann cell proliferation for peripheral nerve repair, Journal of tissue engineering and regenerative medicine 8 (2014), https://doi.org/10.1002/term.1509.

[49] J. Wang, W. Zheng, L. Chen, T. Zhu, W. Shen, C. Fan, H. Wang, X. Mo, Enhancement of Schwann cells function using graphene-oxide-modified nanofiber scaffolds for peripheral nerve regeneration, ACS Biomater. Sci. Eng. 5 (2019), https://doi.org/10.1021/acsbiomaterials.8b01564.

[50] Y. Qian, Z. Yao, X. Wang, Y. Cheng, Z. Fang, W.-E. Yuan, C. Fan, Y. Ouyang, (-)-Epigallocatechin gallate-loaded polycaprolactone scaffolds fabricated using a 3D integrated moulding method alleviate immune stress and induce neurogenesis, Cell Prolif 53 (1) (2020), e12730, https://doi.org/10.1111/cpr.12730.

[51] N. de la Oliva, X. Navarro, J. del Valle, Time course study of long-term biocompatibility and foreign body reaction to intraneural polyimide-based implants, J. Biomed. Mater. Res. 106 (3) (2018) 746–757, https://doi.org/10.1002/jbm.a.36274.

[52] Y. Yao, L. Bian, P. Yang, Y. Sui, R. Li, Y. Chen, L. Sun, Q. Ai, L. Zhong, D. Lu, Gastrodin attenuates proliferation and inflammatory responses in activated microglia through Wnt/β-catenin signaling pathway, Brain Res. 1717 (2019) 190–203, https://doi.org/10.1016/j.brainres.2019.04.025.

[53] M.A. Oliveira, L. Heimfarth, F.R.S Passos, M.R. Miguel-dos-Santos, J.C.F. Moreira, S.S. Lauton, R.S.S. Barreto, A.A.S. Araújo, A.P. Oliveira, J.T. Oliveira, A.F. Baptista, A.M.B Martinez, L.J. Quintans-Júnior, J.S.S. Quintans, Naringenin complexed with hydroxypropyl-β-cyclodextrin improves the sciatic nerve regeneration through inhibition of p75NTR and JNK pathway, Life Sci. 241 (2020) 117102, https://doi.org/10.1016/j.lfs.2019.117102.

[54] H. Neumann, R. Schweigreiter, T. Yamashita, K. Rosenkranz, H. Wekerle, Y.-A. Barde, Tumor necrosis factor inhibits neurite outgrowth and branching of hippocampal neurons by a rho-dependent mechanism, J. Neurosci. : the official journal of the Society for Neuroscience 22 (3) (2002) 854–862, https://doi.org/10.1523/JNEUROSCI.22-03-00854.2002.

[55] A.L. Kalinski, C. Yoon, L.D. Huffman, P.C. Duncker, R. Kohen, R. Passino, H. Hafner, C. Johnson, R. Kawaguchi, K.S. Carbajal, J.S. Jara, E. Hollis, D. H. Geschwind, B.M. Segal, R.J. Giger, Analysis of the immune response to sciatic nerve injury identifies efferocytosis as a key mechanism of nerve debridement, Elife 9 (2020), https://doi.org/10.7554/eLife.60223.

[56] X. Feng, Y. Takayama, N. Ohno, H. Kanda, Y. Dai, T. Sokabe, M. Tominaga, Increased TRPV4 expression in non-myelinating Schwann cells is associated with demyelination after sciatic nerve injury, Commun Biol 3 (1) (2020), https://doi.org/10.1038/s42003-020-01444-9, 716-716.

[57] S.E. Park, J. Ahn, H.-E. Jeong, I. Youn, D. Huh, S. Chung, A three-dimensional in vitro model of the peripheral nervous system, NPG Asia Mater. 13 (1) (2021), https://doi.org/10.1038/s41427-020-00273-w.

[58] Q. Ao, C.-K. Fung, A. Yat-Ping Tsui, S. Cai, H.-C. Zuo, Y.-S. Chan, D. Kwok-Yan Shum, The regeneration of transected sciatic nerves of adult rats using chitosan nerve conduits seeded with bone marrow stromal cell-derived Schwann cells, Biomaterials 32 (3) (2011) 787–796, https://doi.org/10.1016/j.biomaterials.2010.09.046.

[59] T. Saffari, M. Bedar, C. Hundepool, A. Bishop, A. Shin, The role of vascularization in nerve regeneration of nerve graft, Neural Regen Res 15 (2020) 1573, https://doi.org/10.4103/1673-5374.276327.